Production of Λ hyperons in interactions of the 4A GeV carbon beam with *C*, *Al*, *Cu* targets

A.Zinchenko, Yu.Gornaya, M.Kapishin, G.Pokatashkin, I.Rufanov, V.Vasendina

for the BM@N collaboration

VBLHEP, JINR, Dubna, Russia

Joint Institute for Nuclear Research
SCIENCE BRINGING NATIONS TOGETHER

BM@N collaboration analysis meeting
30.05.2019

Outline

1. Technical run with carbon beam (March 2017)
   - ✓ BM@N detector set-up
2. Data analysis (*C*+*C*, *C*+*Al*, *C*+*Cu* at 4A GeV)
   - ✓ Selection criteria
   - ✓ Reconstructed signal of Λ (dN/dY & dN/p_T spectra)
   - ✓ Data - MC agreement: multiplicity, momentum spectra
   - ✓ Decomposition of Λ reconstruction efficiency
   - ✓ Trigger and mean impact parameters
   - ✓ Cross section and yields of Λ
   - ✓ Reconstructed p_T spectra of Λ and extracted temperature
   - ✓ Systematic errors and extrapolation factors
3. Summary and plans

BM@N set-up in carbon run

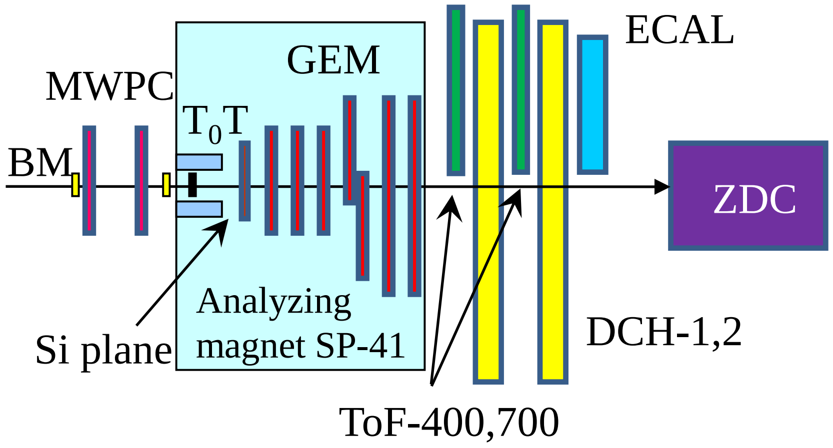

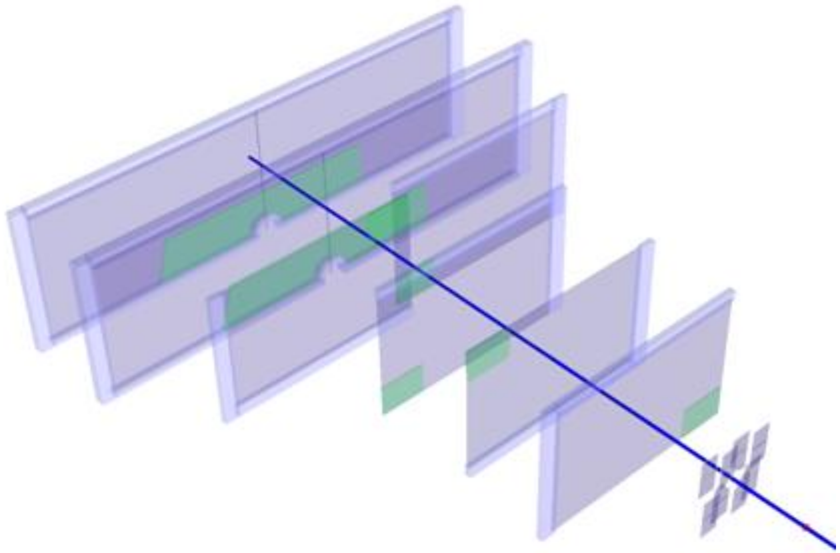

Central tracker in carbon run.

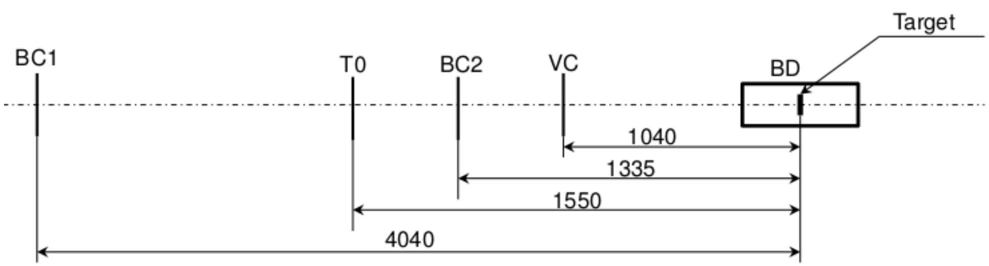

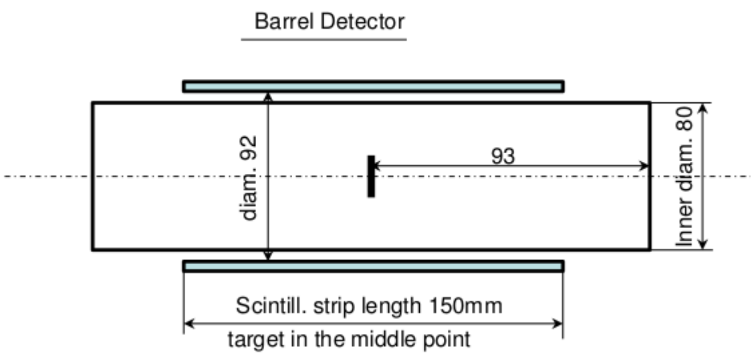

Schematic view and positions of the beam counters, barrel detector and target.

Event selection criteria

- ✓ Number of tracks in selected events: pos>=1, neg>=1;
- ✓ Beam halo, pile-up suppression within the readout time window: number of signals in the start detector: T0=1, number of signals in the beam counter: BC2=1, number of signals in the veto counter around the beam: Veto=0;
- ✓ Trigger condition in the barrel multiplicity detector: number of signals BD>=2 or BD>=3 (run dependent).

Cut	1	2	3	4
T0==1	+			+
BC2==1		+		+
VET0==0			+	+
C	77.0	82.7	82.1	67.4
Al	82.4	87.5	86.0	74.0
Cu	86.0	89.1	87.9	77.9
Pb	85.9	89.6	89.2	79.0

Table 1. Number of triggered events, beam fluxes and integrated luminosities collected in the carbon beam of 4A GeV.

Interactions (target thickness)	Number of triggers / 10^6	Integrated beam flux / 10^7	Integrated luminosity / 10^{30} cm^{-2}
C+C (9mm)	4.57	6.99	7.16
C+Al (12mm)	5.35	4.41	3.11
C+Cu (5mm)	5.31	4.57	1.98

Λ hyperon selection criteria

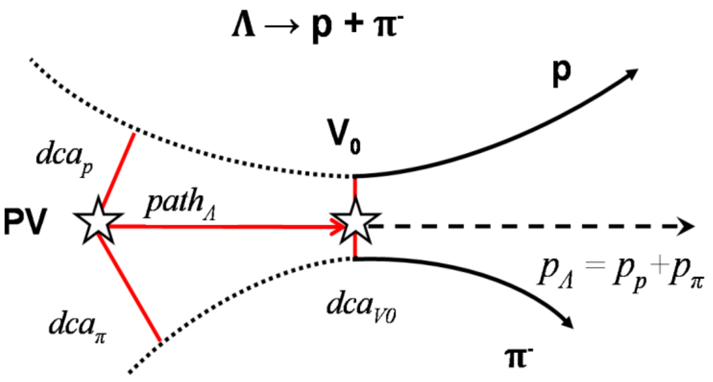

Event topology:

- ✓ PV – primary vertex
- ✓ V_0 – vertex of hyperon decay
- ✓ *dca* – distance of the closest approach
- ✓ *path* – decay length

- ✓ Number of hits in 1 Si + 6 GEM per track > 3
- ✓ Momentum range of positive tracks: $0.5 < p_{pos} < 3.9$ GeV/c
- ✓ Momentum range of negative tracks: $0.3 < p_{neg} < 1.8$ GeV/c
- ✓ Distance of minimum approach of *V0* tracks: *dca* < 1 cm
- ✓ Distance between *V0* and primary vertex: *path* > 2.5 cm

Table2. Reconstructed signals of Λ in p_T and *y* bins.

Target / Interval	*Y* intervals			Target / Interval	p_T intervals		
	C	*Al*	*Cu*		*C*	*Al*	*Cu*
1.2-1.45	103±32	265±54	591±83	0.1-0.3	454±82	652±101	625±103
1.45-1.65	250±52	510±70	601±72	0.3-0.55	296±53	717±96	797±97
1.65-1.85	338±69	550±87	576±93	0.55-0.8	128±37	462±78	379±74
1.85-2.1	253±61	443±87	371±81	0.8-1.05	no	96±47	133±53

Signal of Λ in *C+Cu* interaction

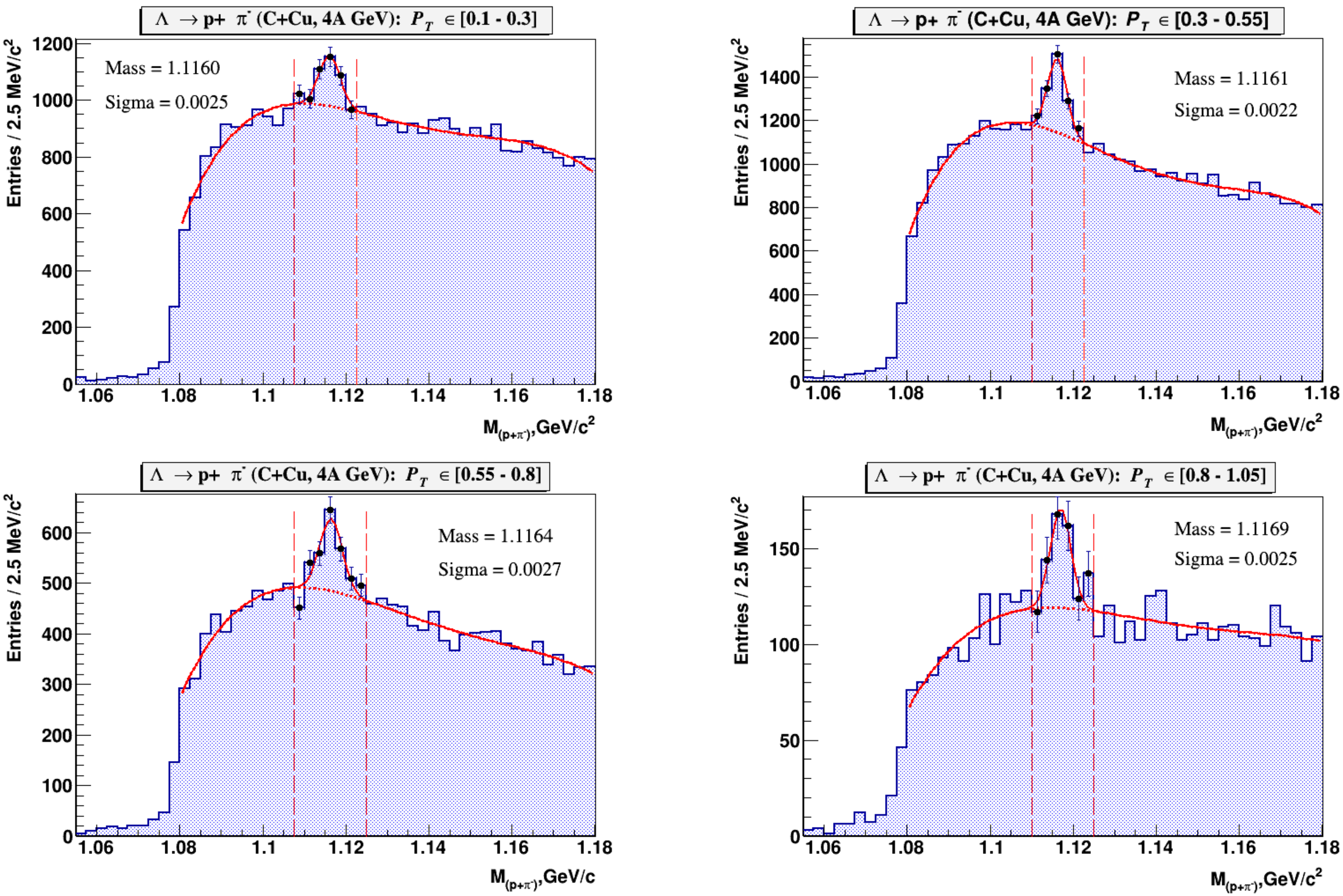

Fig. 4. $\Lambda \to p\pi^-$ signal reconstructed in *C+Cu* interaction in bins of the transverse momentum p_T. The signal is fitted by a Gaussian function, the background is fitted by the 4th degree polynomial.

Signal of Λ in $C+Cu$ interaction

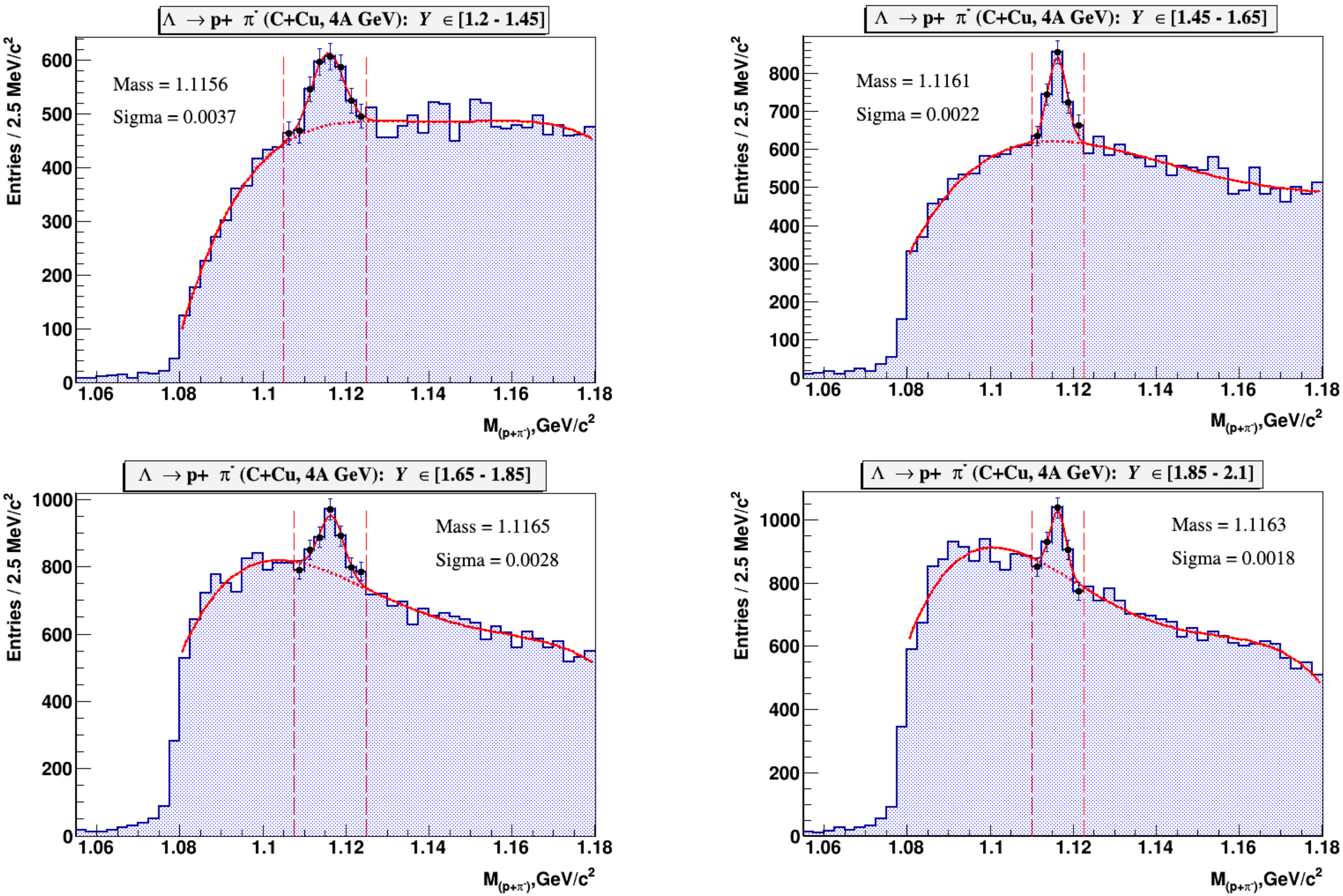

Fig. 7. $\Lambda\rightarrow p\pi^-$ signal reconstructed in $C+Cu$ interaction in bins of the rapidity y. The signal is fitted by a Gaussian function, the background is fitted by the 4th degree polynomial.

Signal of Λ in *C+C*, *C+Al*, *C+Cu* interactions

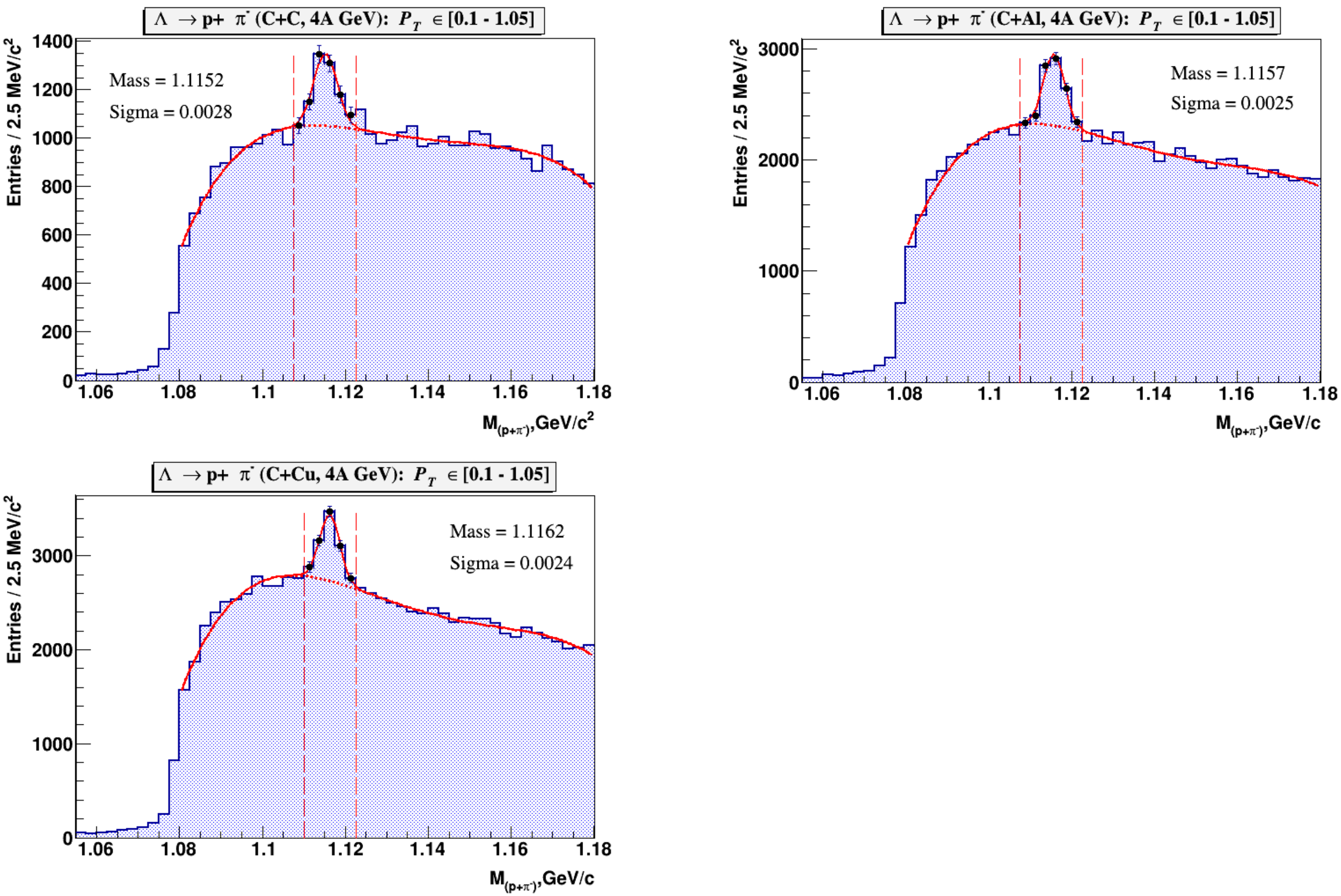

Fig. 8. $\Lambda \rightarrow p\pi^-$ signal reconstructed in interactions of the carbon beam with targets: *C*, *Al*, *Cu*.

Comparison of experimental data and MC

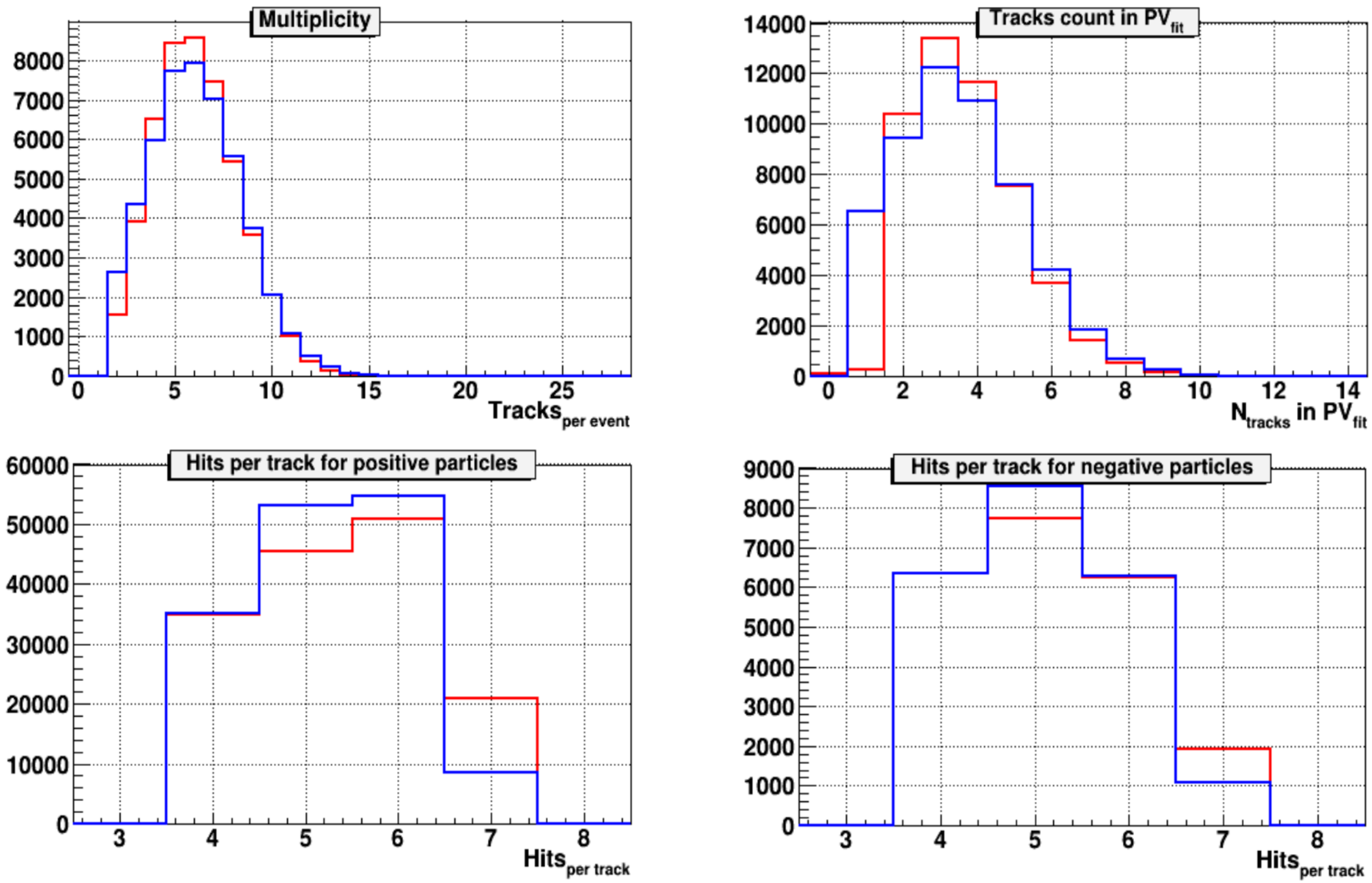

Fig.9. Comparison of experimental distributions (red lines) and MC (DCM-QGSM) (blue curves) in *C+Cu* interaction: track multiplicity per event; number of tracks reconstructed in the primary vertex; number of hits per positive particle reconstructed in 1 Si + 6 GEM detectors; number of hits per negative particle.

Comparison of experimental data and MC

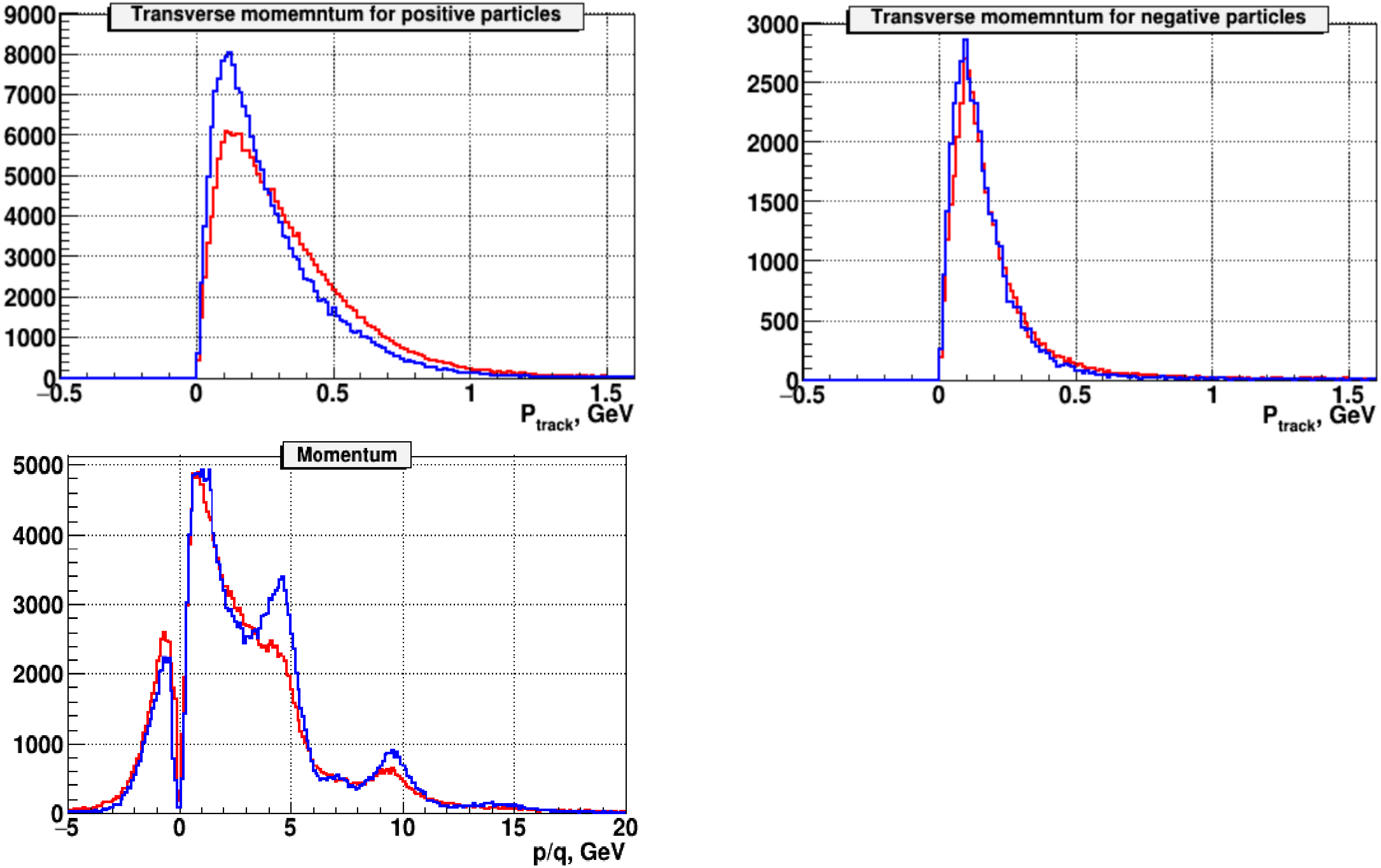

Fig. 10. Comparison of experimental data (red curves) and MC (DCM-QGSM) simulation (blue curves) in *C+Cu* interaction: transverse momentum of positive particles; transverse momentum of negative particles; total momentum of negative (*p/q*<0) and positive particles (*p/q*>0).

Decomposition of efficiency

Table 3. Decomposition of Λ reconstruction efficiency.

Reconstruction efficiency	$\varepsilon_{rec} = \varepsilon_{acc} \cdot \varepsilon_{emb} \cdot \varepsilon_{cuts}$
Λ geometrical acceptance in GEM detectors	$\varepsilon_{acc} = N_{acc}(y,p_T) / N_{gen}(y,p_T)$
Efficiency of reconstruction of embedded Λ	$\varepsilon_{emb} = N_{emb}(y,p_T) / N_{acc}(y,p_T)$
Efficiency of Λ selection: kinematical and spatial cuts	$\varepsilon_{cuts} = N_{rec}(y,p_T) / N_{emb}(y,p_T)$

2-dimentional (p_T,y) distributions of reconstructed Λ decay candidates in data and Monte Carlo do not perfectly agree in the shape. To adjust the Monte Carlo to the data, weights were calculated as a ratio of the normalized spectra of experimental data to the normalized spectra of simulated events: $w(y,p_T) = N_{data}(y,p_T)/N_{rec}(y,p_T)$.

The 2-dimentional weights are shown in Fig.14. These weights were used to obtain 1-dimentional efficiencies according to the formula:

$$\varepsilon_{rec}(p_T) = \Sigma_y(N_{rec}(y,p_T) \cdot w(y,p_T)) / \Sigma_y(N_{gen}(y,p_T) \cdot w(y,p_T))$$

$$\varepsilon_{rec}(y) = \Sigma_{pT}(N_{rec}(y,p_T) \cdot w(y,p_T)) / \Sigma_{pT}(N_{gen}(y,p_T) \cdot w(y,p_T))$$

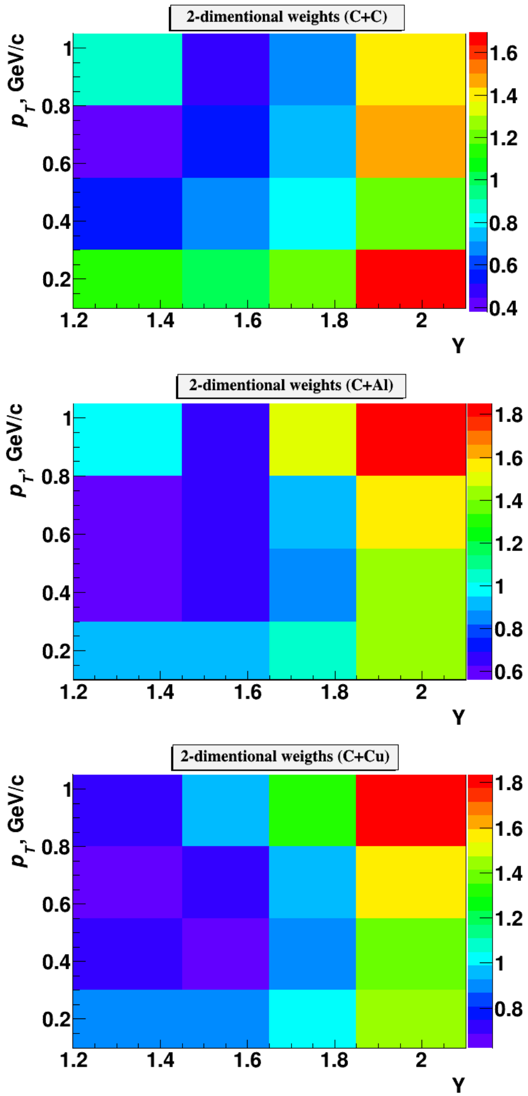

Fig.14. 2-dimentional weights $w(y,p_T)$.

Efficiency in $C+Cu$ interaction

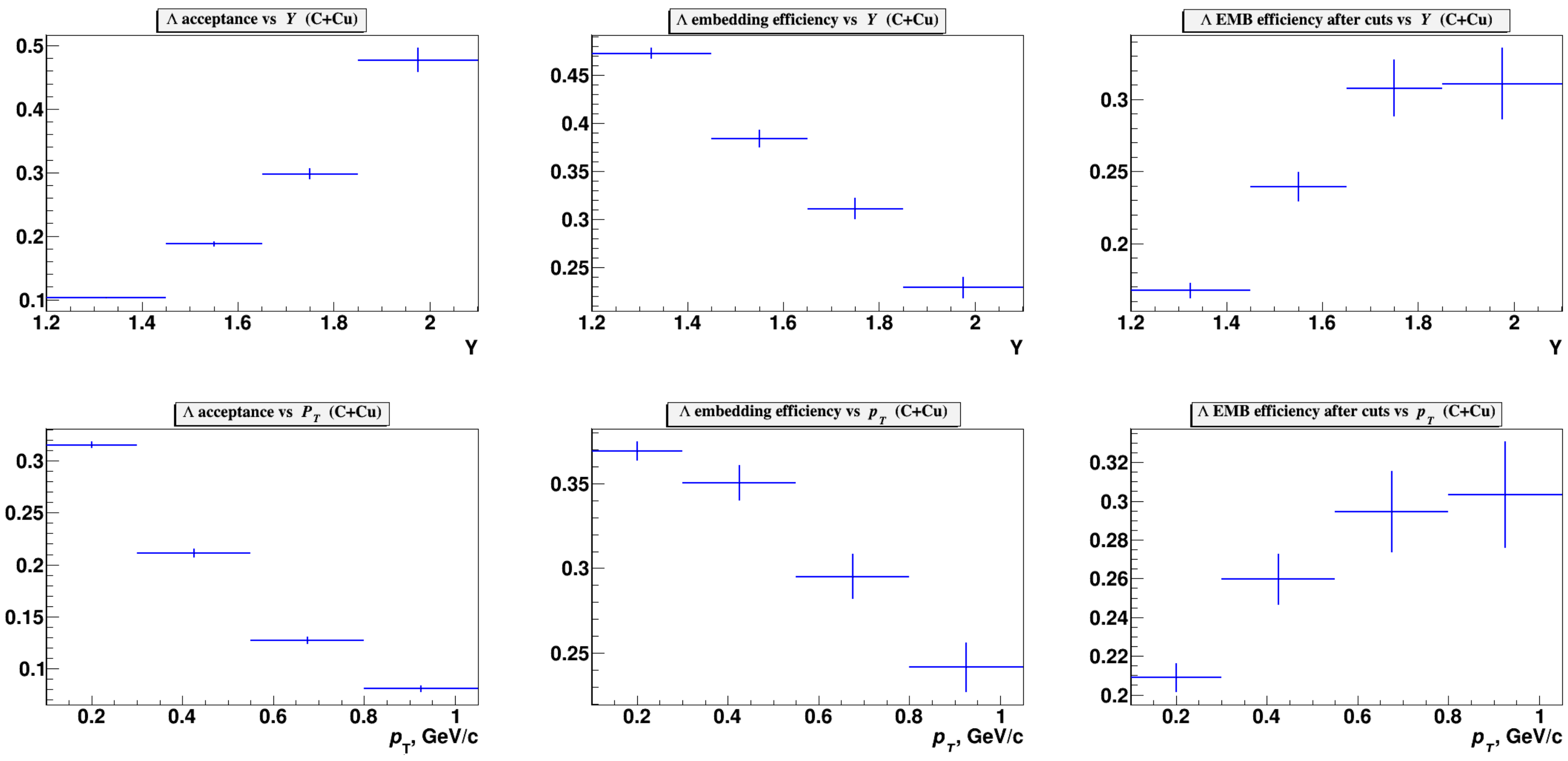

Fig.18. Λ geometrical acceptance (ε_{acc}); efficiency of reconstruction of embedded Λ (ε_{emb}); efficiency of kinematical and spatial cuts applied for Λ reconstruction (ε_{cuts}) as functions of rapidity y (top plots) and p_T (bottom plots). Results are shown for $C+Cu$ interaction.

Triggers and impact parameters

Table 4. Trigger efficiency evaluated for events with reconstructed Λ hyperons in interactions of the carbon beam with *C*, *Al*, *Cu* targets. The systematic errors take into account the uncertainty due to the delta electron background. The last row shows the trigger efficiency averaged over the data samples with trigger conditions BD>=2 and BD>=3.

Trigger / Target	*C*	*Al*	*Cu*
ε_{trig} (BD>=2)	0.906±0.010	0.955±0.010	0.904±0.01
ε_{trig} (BD>=3)		0.923±0.020	0.883±0.02
ε_{trig} averaged		0.940±0.015	0.893±0.015

Table 5. Mean impact parameters of min. bias *C+C*, *C+Al*, *C+Cu* interactions.

MC	*b*, fm (*C+C*)	*b*, fm (*C+Al*)	*b*, fm (*C+Cu*)
All min bias events	3.76	4.36	5.13
Events with gen. Λ	2.80	3.08	3.58
Events with rec. Λ	2.71	3.18	3.88

The Λ yields and production cross section

Table 11.

Interacting nucleus / reference	Beam momentum, kinetic energy (T_0)	Λ cross section, mb	Λ yield, $\cdot 10^{-2}$
He_4+Li_6	4.5 GeV/c (3.66A GeV)	5.9± 1.5	1.85 ± 0.5
$C+C$	4.2 GeV/c (3.36AGeV)	24 ± 4	
$C+C$, propane chamber	4.2 GeV/c (3.36A GeV)		2.8 ± 0.3
$p+p$	4.95 GeV/c (4.1 GeV)		2.3 ± 0.4
$C+C$, HADES	2A GeV	$8.7 \pm 1.1 \pm^{3.2}_{1.6}$	$0.92 \pm 0.12 \pm^{0.34}_{0.17}$
$Ar+KCl$, HADES	1.76AGeV		3.93±0.14±0.15
$Ar+KCl$, FOPI	1.93A GeV		3.9±0.14±0.08
$Ni+Ni$, FOPI, central 390 mb from 3.1 *b*	1.93A GeV		$0.137 \pm 0.005 \pm^{0.009}_{0.025}$
$Ni+Cu$, EOS, full b<8.9 fm / central b<2.4 fm	2A GeV	112±24 / 20±3	
$Ar+KCl$, central b<2.4 fm	1.8A GeV	7.6±2.2	

Cross section and yields of Λ hyperon

The cross section σ_Λ and yield Y_Λ of Λ hyperon production in $C+C$, $C+Al$, $C+Cu$ interactions are calculated in bins of y and p_T according to the formulae:

$$\sigma_\Lambda(y,p_T)=N_{rec}^{\Lambda}(y,p_T) / (\varepsilon_{rec}(y,p_T)\cdot\varepsilon_{trig}\cdot L); \qquad Y_\Lambda(y,p_T) = \sigma_\Lambda(y,p_T) / \sigma_{inel}$$

where L is the luminosity,
N_{rec}^{Λ} – the number of reconstructed Λ hyperons,
ε_{rec} – the combined efficiency of the Λ hyperon reconstruction,
ε_{trig} – the trigger efficiency,
σ_{inel} – the cross section for minimum bias inelastic $C+A$ interactions.

Interaction	***C+C***	***C+Al***	***C+Cu***
Inelastic cross section, mb	830±50	1260±50	1790±50

The cross sections for inelastic $C+Al$, $C+Cu$ interactions are taken from the predictions of the DCM-QGSM model which are consistent with the results calculated by the formula: $\sigma_{inel} = \pi R_0^2 (A_P^{1/3} + A_T^{1/3})^2$, where R_0 = 1.2 fm is an effective nucleon radius, A_P and A_T are atomic numbers of the beam and target nucleus.

Number of reconstructed Λ hyperons

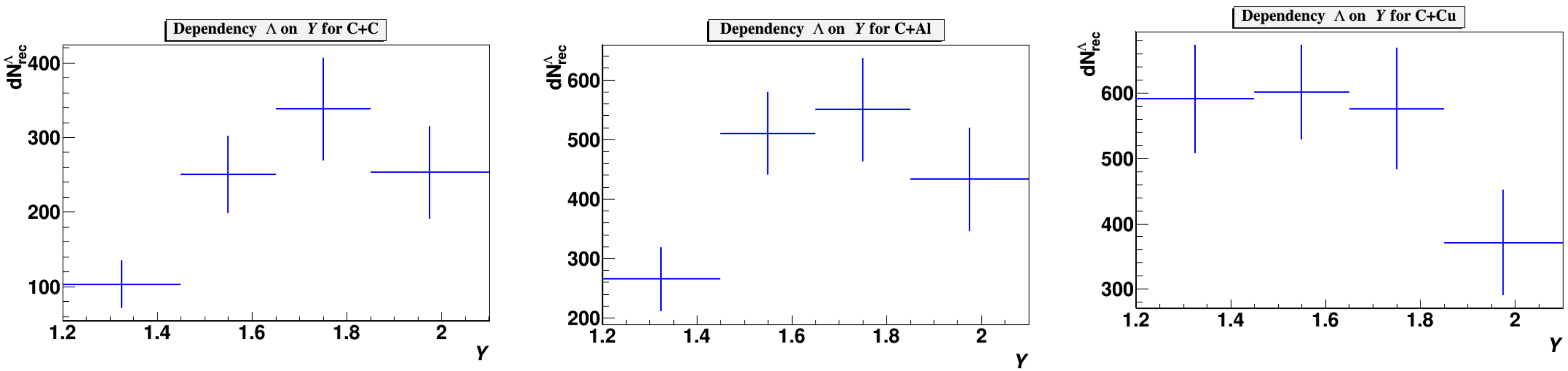

Fig.15. Number of reconstructed *Λ* hyperons in *C+C*, *C+Al*, *C+Cu* data samples in bins of *y*.

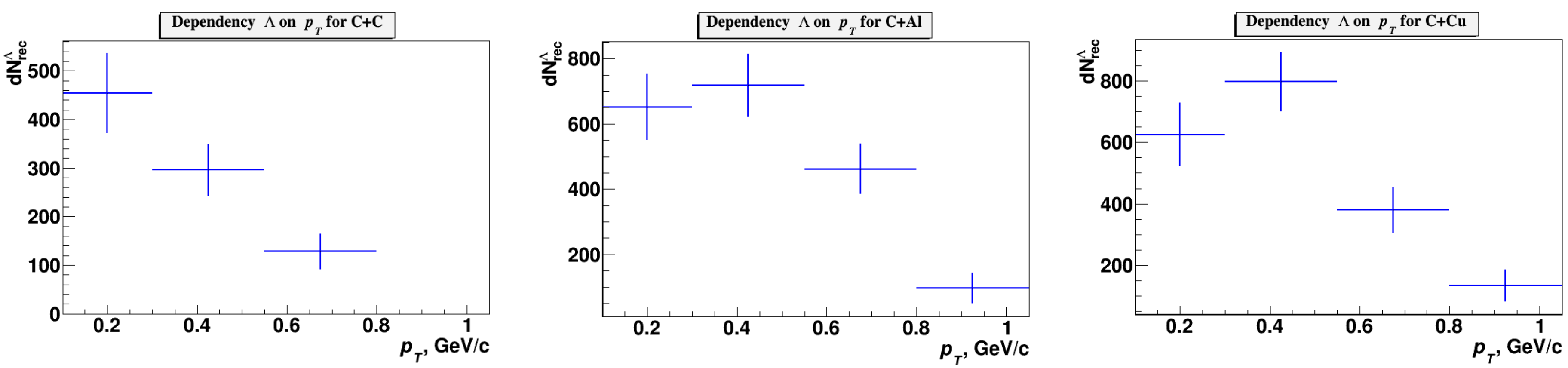

Fig.15. Number of reconstructed *Λ* hyperons in *C+C*, *C+Al*, *C+Cu* data samples in bins of p_T.

Reconstructed yields of Λ hyperons

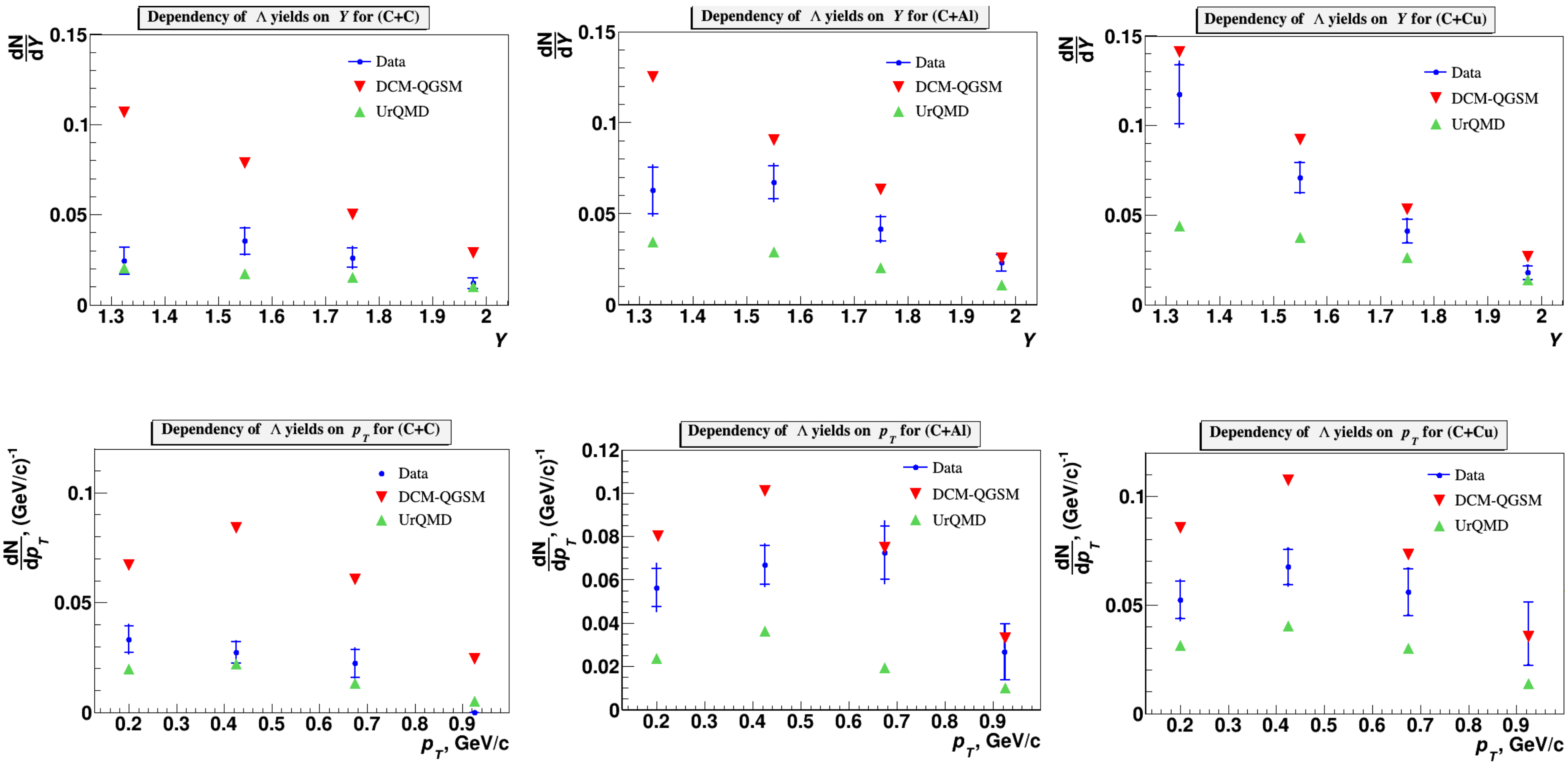

Fig. 20-22. Reconstructed yields of *Λ* hyperons in minimum bias *C+C*, *C+Al*, *C+Cu* interactions vs rapidity *y* and transverse momentum p_T (blue crosses). Predictions of the DCM-QGSM and UrQMD models are shown as red and green crosses.

Reconstructed p_T spectra of Λ and extracted T_0

Table 6. Temperature parameter extracted from the fit of the p_T spectra.

	T_0, MeV (*C+C*)	T_0, MeV (*C+Al*)	T_0, MeV (*C+Cu*)
Experiment	93.7±29.3±12.7	155.0±30.0±19.4	157.6±33.9±9.5
χ^2 /ndf	2.38/1	2.05/2	0.43/2
DCM-QGSM	121.9	129.4	130.5
UrQMD	107.3	126.7	131.8

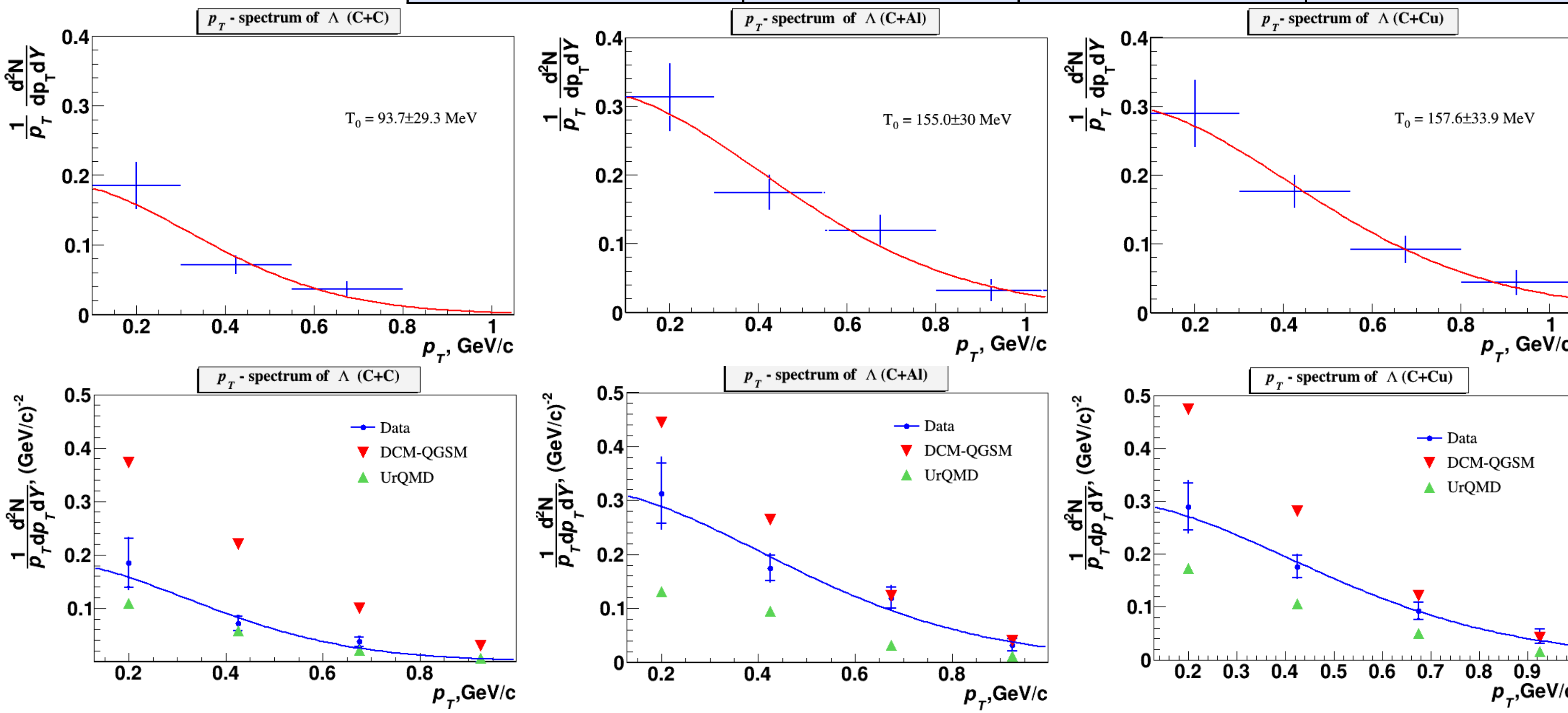

Fig. 23. Thermal fit results with the inverse slope parameter T_0: data and predictions of models.

p_T spectra of Λ: MC predictions

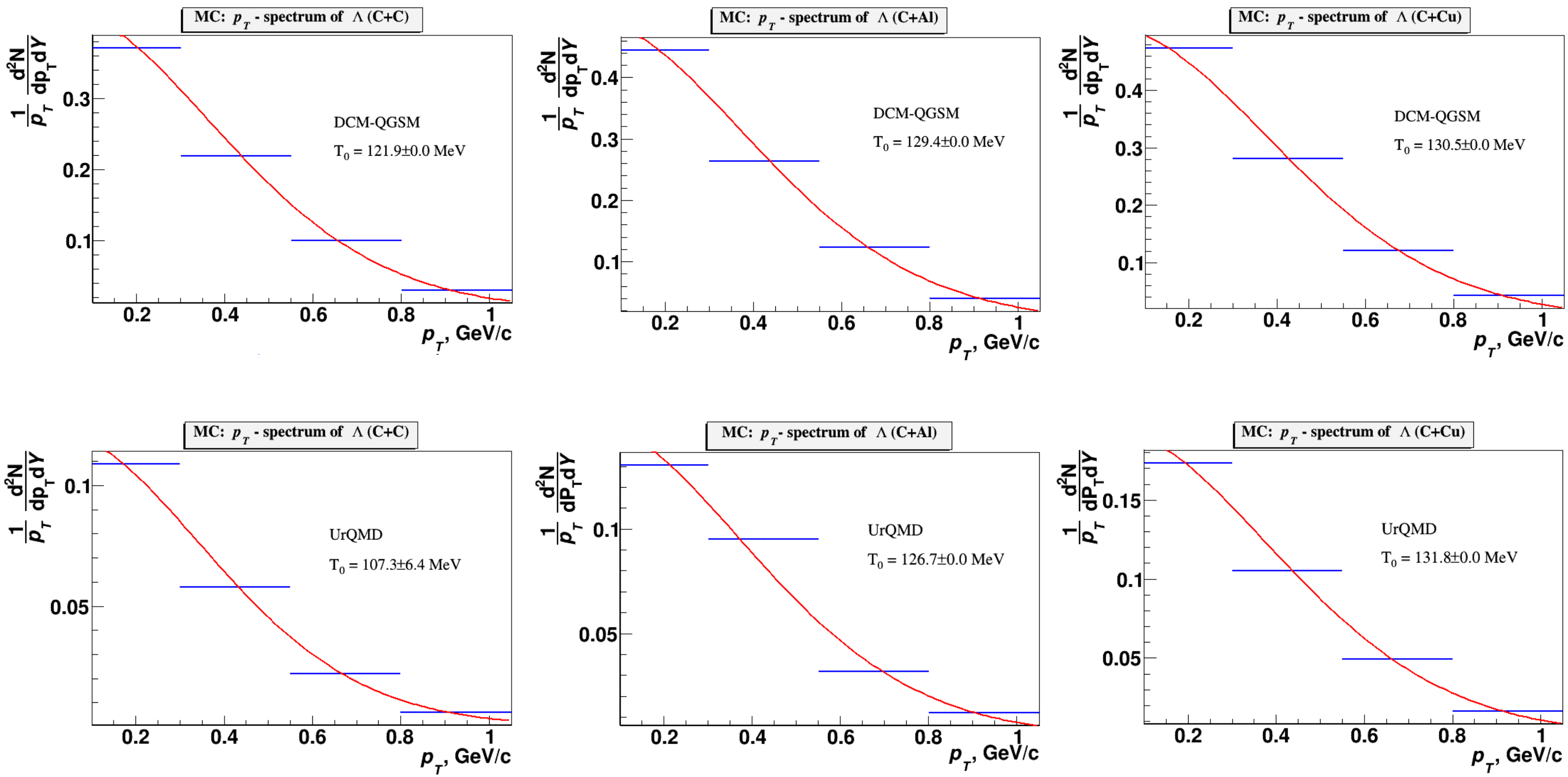

Fig. 24. Fit of the DCM-QGSM and URQMD spectra. The inverse slope parameter T_0 is shown, extracted from the fit.

Systematic errors

The systematic error of the Λ yield in every p_T and y bin is calculated via a quadratic sum of uncertainties coming from the following sources: Systematic errors of the embedding efficiency estimated by embedding the Λ decay products into data samples collected in different run periods;

Table 7. Systematic uncertainty of the embedding efficiency.

Target / Interval	*Y*			Target / Interval	p_T		
	C, sys%	*Al*, sys%	*Cu*, sys%		*C*, sys%	*Al*, sys%	*Cu*, sys%
1.2-1.45	2.09	-4.22	-2.93	0.1-0.3	-4.94	-9.37	-6.61
1.45-1.65	1.75	-4.11	3.31	0.3-0.55	-3.07	0.64	-1.30
1.65-1.85	-7.96	-4.78	-4.19	0.55-0.8	-4.59	0.34	0.078
1.85-2.1	-5.44	-1.24	-6.09	0.8-1.05	3.03	-6.28	-2.36

Systematic errors estimated by two methods of reweighting the Monte Carlo (y,p_T) distribution to adjust it to the measured (y,p_T) distribution: 1) using 2-dimentional weight $w(y,p_T)$ in the measured (y,p_T) bin; 2) using product of 1-dimentional weights calculated as $w(p_T)\cdot w(y)$.

Table 8. Systematic uncertainty of the total reconstruction efficiency.

Target / Interval	*Y*			Target / Interval	p_T		
	C, sys%	*Al*, sys%	*Cu*, sys%		*C*, sys%	*Al*, sys%	*Cu*, sys%
1.2-1.45	7.39	8.50	6.57	0.1-0.3	8.70	8.20	5.85
1.45-1.65	7.80	6.39	3.40	0.3-0.55	7.14	6.05	5.21
1.65-1.85	9.08	7.60	4.26	0.55-0.8	11.23	10.48	3.19
1.85-2.1	7.34	7.35	5.01	0.8-1.05	2.06	7.16	2.32

Systematic errors

Table 9. Total systematic uncertainty.

Target / Interval	*Y*			Target / Interval	p_T		
	C, sys%	***Al***, sys%	***Cu***, sys%		***C***, sys%	***Al***, sys%	***Cu***, sys%
1.2-1.45	±7.68	±9.48	±7.19	0.1-0.3	±10.00	±12.45	±8.82
1.45-1.65	±7.99	±7.60	±4.74	0.3-0.55	±7.77	±6.08	±5.36
1.65-1.85	±12.07	±8.97	±5.97	0.55-0.8	±12.13	±10.48	±3.19
1.85-2.1	±9.14	±7.45	±7.88	0.8-1.05	±3.66	±9.52	±3.31
Normalization	±6.0	±4.0	±2.8	Normalization	±6.0	±4.0	±2.8

Extrapolation factors

Table 10. Extrapolation factors to the full kinematic range, yields and cross sections.

	C	*Al*	*Cu*
DCM-QGSM URQMD extrapolation factors	6574/2474 1827/639	10539/3413 3248/1056	15817/3545 5509/1360
Yields in the measured kinematic range $0.1<p_T<1.05$ GeV/c, $1.2<y_{lab}<2.1$	0.0190±0.0022±0.0036	0.0528±0.0045±0.0098	0.0503±0.0042±0.0062
Yields in the full kinematic range	0.0524±0.0062±0.0100	0.163±0.014±0.030	0.214±0.018±0.026
Λ cross section in min. bias interactions, mb	41.9±4.9±7.7	205.0±17.6±37.4	383.2±31.5±49.2

Summary

1. Production of Λ hyperons in interactions of the 4A GeV kinetic energy carbon beam with *C*, *Al*, *Cu* targets was studied with the BM@N detector at the Nuclotron.
2. The analysis procedure has been presented and described.
3. Results on Λ hyperon yields have been obtained and compared with model predictions and data available.
4. Request for BM@N preliminary.

Thank you for attention!

Backup

Residual distributions of GEM hits

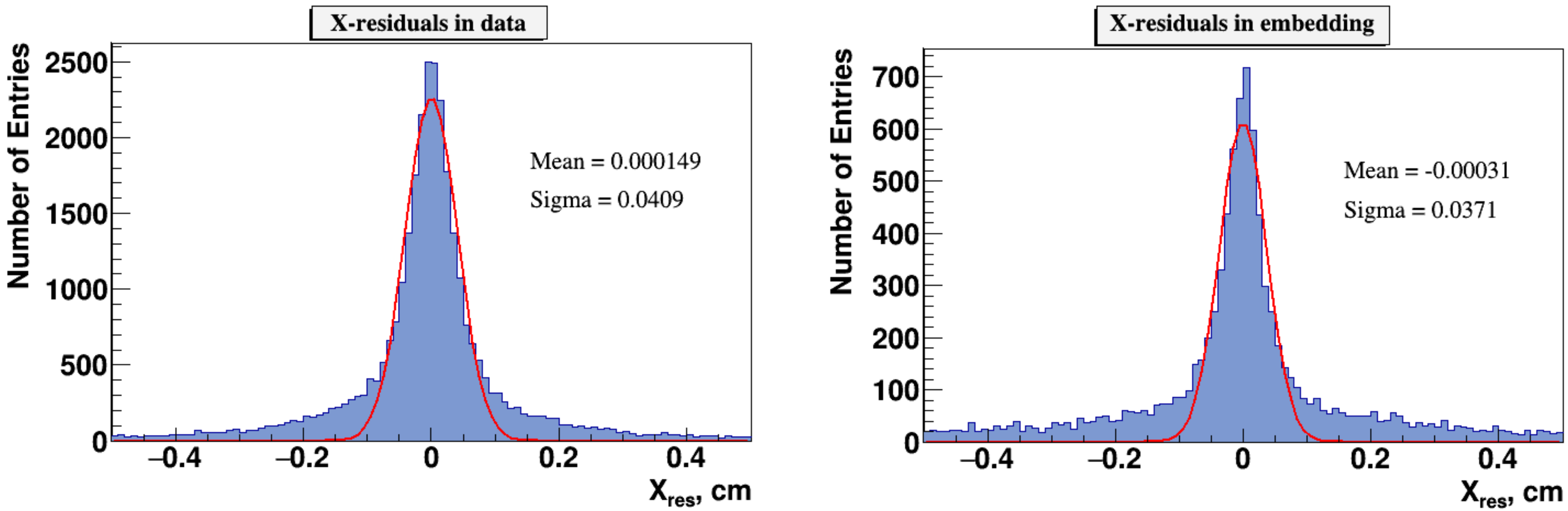

Fig. 12. Residual distributions of GEM hits with respect to reconstructed tracks: left) experimental data, right) reconstructed tracks of embedded *Λ* decay products.

DCA and PV position

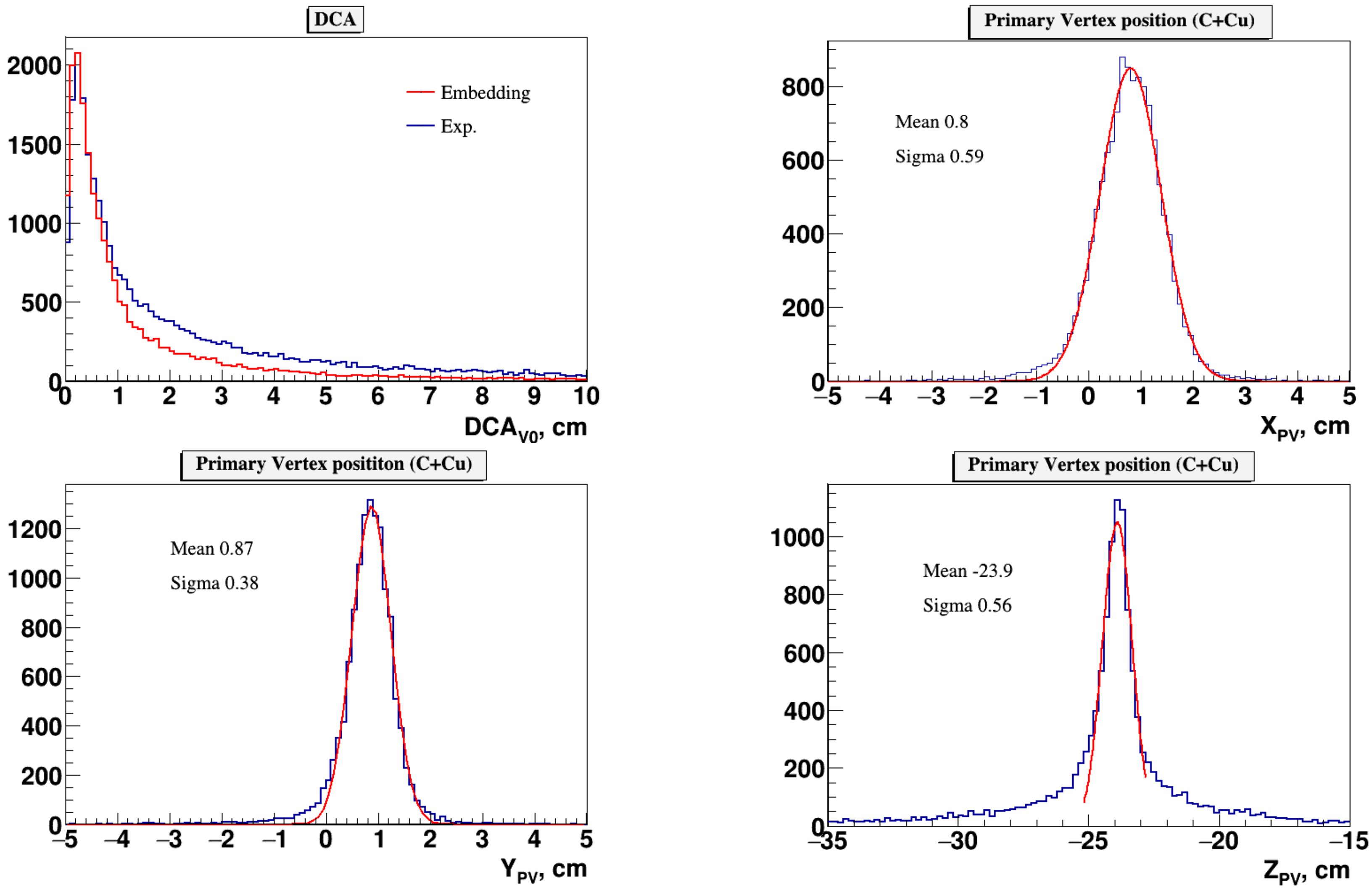

Fig. 12b. Distance of the closest approach of *V0* decay tracks (*DCA*) and *Z*,*X*,*Y* distributions of the primary vertex.

The invariant mass spectrum

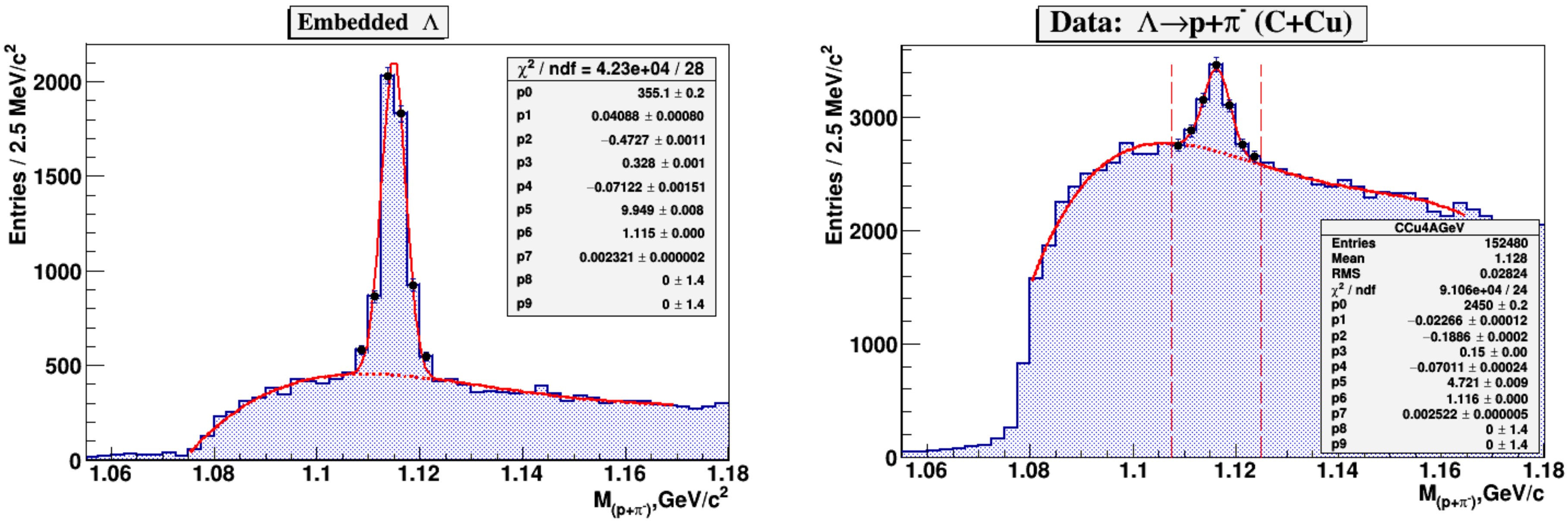

Fig. 13. The invariant mass spectrum of (p,π^-) pairs reconstructed in the experimental events of *C+Cu* interactions with embedded *Λ* hyperon decay products (left); The invariant mass spectrum of (p,π^-) pairs reconstructed in *C+Cu* interactions (right).

Efficiency distributions in GEMs

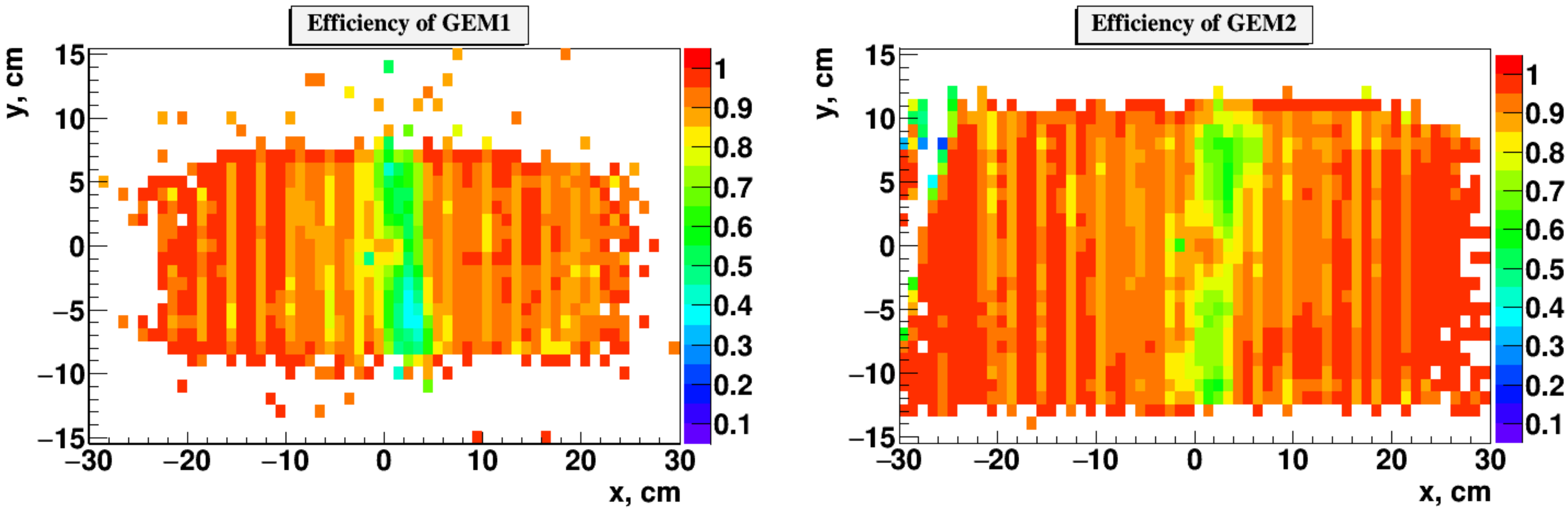

Fig. 11. Two-dimensional *X/Y* efficiency distributions in 6 GEM stations measured with experimental tracks and implemented into Monte Carlo simulation.